Calcium-Dependent Stability Studies of Domains 1 and 2 of Epithelial Cadherin†

Alka Prasad and Susan Pedigo*

Department of Chemistry and Biochemistry, University of Mississippi, University, Mississippi 38677

Received May 31, 2005; Revised Manuscript Received August 8, 2005

ABSTRACT: Epithelial cadherin is important in establishing and maintaining cell to cell interactions in epithelial cells, thereby playing an important role during morphogenesis. The epithelial cadherin molecules have three main regions: the N-terminal extracellular region, the transmembrane region that spans the cell membrane once, and the C-terminal cytoplasmic region that communicates with the cytoskeletal actin filaments through catenins. We report studies of the calcium-dependent stability of extracellular domains 1 and 2 of epithelial cadherin as a two-domain construct (MECAD12). Circular dichroism (CD) spectra of MECAD12 indicated a typical β-sheet conformation in all solution conditions. Thermal- and denaturant-induced unfolding was monitored by CD. Distinct calcium stabilization was observed as a shift in T_m from 40 (apo) to 65 °C (10 mM Ca^{2+}). Spectroscopic experiments agreed well with calorimetric (DSC). In the absence of calcium, the unfolding transition was shallow ($\Delta H_m = 40$ kcal/mol) but not obviously three state. Model-dependent analysis indicated that a second transition could be assigned to the unfolding of domain 2. A calcium-binding constant was derived from the calcium-dependent shift in temperature denaturation profiles. The K_d that was obtained (55 μM) was consistent with literature values. Thus, the modular domains of epithelial cadherin exhibit context-dependent behavior in both the apo and calcium-bound states. This cooperativity between the modules is consistent with the physiological role of epithelial cadherin in signal transduction through cell-adhesive contacts.

Cadherins are a family of transmembrane proteins that are responsible for communication between identical cells mediated by calcium-dependent homophilic interactions (*1*−*4*). In general, proteins belonging to the cadherin family have a common domain organization (*5*−*7*). They contain an amino-terminal extracellular region, a single pass transmembrane region, and a carboxyl-terminal cytoplasmic region, which interacts with the cytoskeleton. The extracellular region of classical cadherins has five homologous and independently folded domains. These domains exhibit homophilic cis and trans interactions (*4*, *7*). Cis dimerization occurs between cadherin molecules emanating from the same cell surface. Trans interactions occur between the N-terminal domains of cadherin molecules originating from opposing cells and are the basis for adhesion (*8*, *9*). Calcium ions bind at the interface between extracellular domains creating a cooperative unit that transduces the adhesive signal to the cytoskeletal network (*10*). Adhesion causes tension in the cytoskeletal network (*11*) leading to downstream signaling events mediated by β-catenin (*12*−*14*).

Studies of cadherin have fallen primarily into two broad categories: high-resolution structural studies and low-resolution cell adhesion studies. Each has its benefits. Solution (*15*−*19*) and crystal (*8*, *20*−*23*) structures of the extracellular domains of cadherins illustrate their modular structure (Figure 1A). The modular domains are seven-strand β-sheet structures with a typical immunoglobulin-type, "Greek key" topology (*24*−*29*). These studies provide evidence of the importance of residues for calcium binding as indicated from mutagenesis. Interestingly, these high-resolution structures displayed a diverse range of cis and trans interactions that are not in agreement with each other (*8*, *19*−*23*). Hence, there is obvious promiscuity in the interactions of these extracellular domains that contrasts with the apparent specificity of their associations in vivo (*30*, *31*). The studies reported here provide a thermodynamic approach as an alternative to the structural studies.

Given that the extracellular domains are modular in nature, it is important for these modules to communicate in order to transduce the signal of the presence of a neighboring cell to the actin cytoskeleton. The modules of cadherin are integrally connected through interactions with calcium ions that bind at the interface between the domains. All three calcium ions that bind at the interface are chelated, in part, by side chain and backbone oxygens from the linker region (consensus sequence DXNDNXP; Figure 1B). The term "linker" illustrates the integral role that this segment plays in the interactions between two adjacent domains or cooperativity between domains. The sequences PENE (10−13), LDRE (66−69), and DAD (134−136) are conserved within the family and are critical for calcium binding (*1*, *8*, *15*, *32*). Calcium binding leads to rigidification of the extracellular region into a stable curved structure (*20*, *33*). This is followed by cis dimerization and trans interactions (*9*, *21*). One might reasonably argue that calcium ion binding transforms the modular extracellular domains into one cooperative unit.

Despite the structural and adhesion studies, the interactions of the extracellular domains of epithelial cadherin remain unclear. To complement information gained from the structural studies, we use an energetic approach to understand folding, calcium binding, and assembly of higher order

† This study was supported by Grant MCB 0212669 from the National Science Foundation.

* To whom correspondence should be addressed. E-mail: spedigo@olemiss.edu. Phone: 662-915-5328. Fax: 662-915-7300.

10.1021/bi0510274 CCC: $30.25
Published on Web 10/01/2005

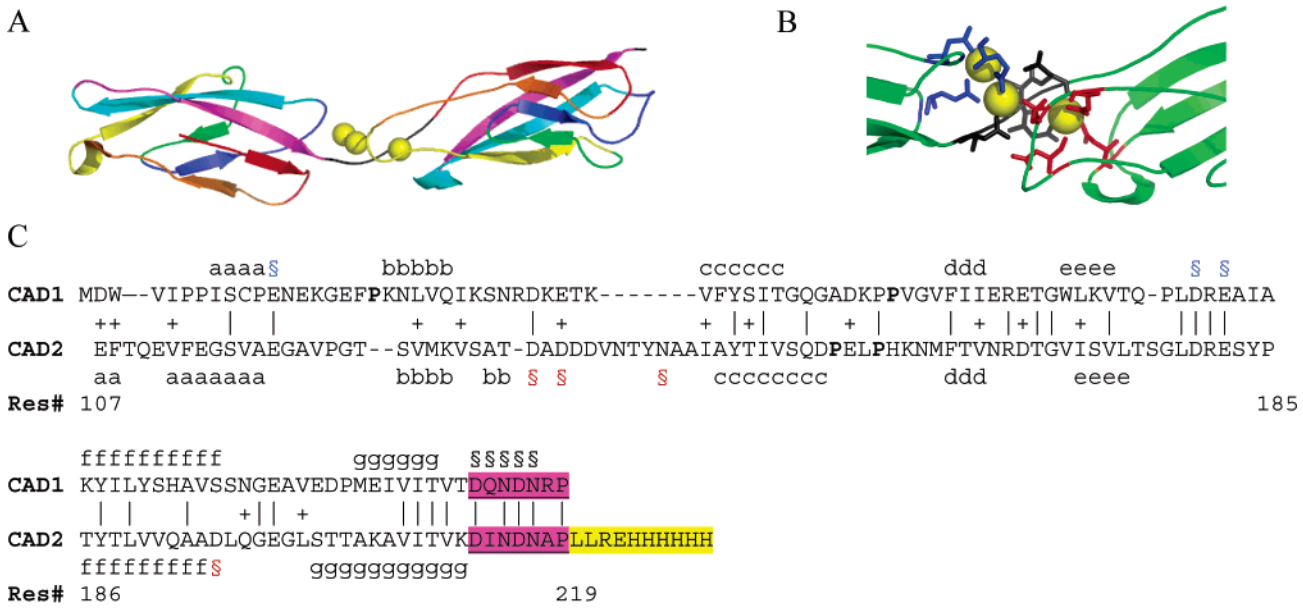

FIGURE 1: Structure and sequence of MECAD12. (A) Ribbon drawing of MECAD12 (*8*) made in PyMOL (www.pymol.org). Sheet regions in each of the domains are colored as follows: sheet a, red; sheet b, orange; sheet c, yellow; sheet d, green; sheet e, blue; sheet f, cyan; sheet g, magenta. Linker 1 and linker 2 are in black; calciums are shown as yellow spheres. (B) Calcium-binding region between two domains. Side chains of residues involved in calcium binding are highlighted in blue (domain 1), black (linker 1), or red (domain 2). (C) Amino acid sequence of MECAD12 with domains aligned to illustrate similar (+) and identical (|) amino acids in the two domains. Lower case letters (a−g) above or below the sequence represent the hydrogen-bonded residues in the β-sheet regions [PROCHECK (*62*)]. Residues involved in binding calcium at the interface between domains 1 and 2 are marked with the symbol § and colored blue (domain 1), black (linker 1), or red (domain 2). Residues highlighted in pink are the linker regions. Residues highlighted in yellow are the N-terminal methionine and the additional residues and the His-tag affinity label. Bolded prolines are in *cis*-X-Pro bonds.

structures (cis and trans interactions). Since domains 1 and 2 are essential for adhesion, we use these as our model system to study these properties. We have taken a reductionist approach and studied the modular domains individually (*34*, *35*). The work presented here examines the calcium-dependent stability of the two-domain construct, MECAD12.[1] Experiments address the energetics of cooperativity between the domains using standard methods for protein denaturation. These studies illustrate that there are energetic consequences of interactions between the domains both in the presence and in the absence of calcium.

MATERIALS AND METHODS

Overexpression and Purification. The MECAD12 clone was provided by Dr. J. Engel (Biocenter, Basel, Switzerland) in pET-22b vector that coded residues from 1 to 219 amino acids of the native protein from mouse epithelial cells (domains 1 and 2). The clone has an N-terminal methionine and a histidine affinity sequence at the C-terminus of linker 2 with four extra amino acid residues in addition to six histidine residues (LLREHHHHHH). This gene was sequenced to confirm the absence of mutations. For the purposes of our work, we define the following domain boundaries. Domain 1 is the most N-terminal extracellular domain comprised of residues 1−99. Domain 2 has residues from 107 to 212. Domains are linked by conserved seven-residue segments known as "linkers". Linker 1 (residues 100−106) connects domain 1 to domain 2. Linker 2 (residues 213−219) connects domain 2 to domain 3. The construct used in the structure determined by Nagar et al contains domain 1, linker 1, domain 2, and linker 2 (Figure 1C). MECAD12 was overexpressed using the BL21(DE3) expression cell line in 1 L volumes each inoculated with 5 mL of a 50 mL overnight culture with 100 μg/mL ampicillin. Cultures were grown at 37 °C to an OD_{600} of ∼1.0 and then induced with 0.4 mM IPTG. The cells were harvested by centrifugation 2 h post induction and frozen at −20 °C. The pellet from 3 L was resuspended in ∼30 mL of 0.5 mM EDTA. The resuspended pellet was taken through three cycles of freeze (−70 °C) and thaw (4 °C). This was followed by sonication for 2 min (2 s on and 2 s off). After DNase was added to 0.05 mg/mL and $MgCl_2$ to 1 mM, the sample was incubated at room temperature for 20 min. It was then centrifuged at 10000 rpm at 4 °C for 20 min. MECAD12 was found in the insoluble inclusion body pellet. The pellet was then dissolved in 10% Triton X-100 and incubated at room temperature for 15 min. It was centrifuged again at 10000 rpm at 4 °C for 20 min. The pellet from centrifugation was resuspended in 1% Triton X-100 and mixed well. This was followed by recentrifugation at 10000 rpm at 4 °C for 20 min. The pellet was resuspended in urea buffer (6 M urea, 10 mM potassium phosphate, 1 mM DTT, 140 mM NaCl, pH 7.5). This suspension was then taken through two steps of chromatography. The first step was NTA-Ni affinity chromatography (5 mL column; Pharmacia). The protein was eluted with 20 mM potassium phosphate, 140 mM NaCl, and 300 mM imidazole, pH 8.2. The elution fractions containing MECAD12 were dialyzed in 140 mM NaCl, 2 mM HEPES, 0.1 mM DTT, and 5% glycerol, pH 7.4. The dialyzed protein was chromatographed on Superose 12 (10/

[1] Abbreviations: ECAD2, epithelial cadherin domain 2; L1-ECAD2-L2, epithelial cadherin linker 1 + domain 2 + linker 2; MECAD12, epithelial cadherin domain 1 + linker 1 + domain 2 + linker 2; CD, circular dichroism; OD, optical density; DSC, differential scanning calorimetry; HEPES, *N*-(2-hydroxyethyl)piperazine-*N*′-2-ethanesulfonic acid; IPTG, isopropyl β-D-thiogalactoside; Tris, tris(hydroxymethyl)-aminomethane.

30; Pharmacia) in 140 mM NaCl, 2 mM HEPES, and 0.1 mM DTT, pH 7.4, to remove remaining impurities. Protein stock was aliquoted and stored at −20 °C.

MECAD12 was also prepared from an expression system that yielded soluble protein for which refolding from urea was not required. Protein from this alternative preparation was not frozen before analysis and did not contain a His tag at the C-terminus. This soluble MECAD12 was analyzed to see if refolding of protein stocks during the purification procedure, freezing of stocks, or the presence of the affinity label impacted measurements on the protein. There was no quantitative or qualitative difference in temperature-denaturation experiments with protein from the two preparations. Thus, the agreement in the two preparations provided confirmation that the preparation from an insoluble fraction, the presence of the C-terminal affinity tag, and the storage of protein at −20 °C did not compromise the protein.

Spectral Characterization. A UV scan of purified protein was taken on a Cary 50 Bio UV−vis spectrophotometer in order to determine the stock concentration using a 4 mm quartz cuvette. UV−vis scans were taken in both the absence (10 μM EGTA) and presence (1 mM added calcium) of calcium. Wavelength scans were performed on the Aviv Model 202SF circular dichroism (CD) spectrometer. CD scans in the presence and with no addition of calcium were performed from 200 to 300 nm with a 15 s averaging time. The protein concentration was 16 μM with a path length of 0.2 mm in 140 mM NaCl and 2 mM HEPES, pH 7.4.

Determination of the Molar Absorption Coefficient. Molar absorption of the purified protein was determined in the presence and absence of calcium (*36*, *37*). Briefly, protein was denatured in 8 M GdnHCl and 30 mM MOPS, pH 7.5, and scanned in a UV−vis spectrometer. The stock protein concentration in the denatured state was calculated using an ϵ_{278} based on the number of tryptophan and tyrosine residues in MECAD12. This stock concentration was then used to determine the ϵ_{278} value of the native protein. These experiments were performed in the apo condition with 10 μM EGTA and in the presence of calcium ranging from 1 μM to 10 mM (scans not shown). A value of 23700 ± 1000 M^{-1} cm^{-1} was obtained. The value did not vary systematically with calcium level.

Unfolding Studies: Temperature Denaturation. (A) Temperature-Induced Unfolding As Monitored by CD. CD experiments were performed on an AVIV Model 202SF CD spectrometer. Wavelength scans of protein and buffer were made before each unfolding experiment. The buffer for the apo condition was 140 mM NaCl, 2 mM HEPES, 20 μM EGTA, and 1 mM DTT, pH 7.4. The calcium concentrations used in the buffer were 0 M (10 μM EGTA), no addition (1 μM contaminating calcium), and 100 μM, 1mM, and 10 mM added $CaCl_2$. The temperature ramp rate was set at 1 °C/min with data taken every degree. The temperature range was from 15 to 85 °C. The acquisition time was 5 s. All temperature denaturation experiments were done using a quartz cuvette with a 1 cm path length. The cuvette was fitted with a screw top to prevent evaporation of the solution at high temperatures. The temperature probe was inserted through the cuvette screw top. All of the measurements were made at 222 nm to increase the signal-to-noise ratio.

Temperature-induced unfolding experiments were also performed in the presence of urea at concentrations 0, 0.2, 0.4, 0.6, and 0.8 M for the apo condition (140 mM NaCl, 2 mM HEPES, 1 mM TCEP, 10 μM EGTA). In the presence of calcium (140 mM NaCl, 2 mM HEPES, 1 mM TCEP, 1 mM Ca^{2+}), the urea concentrations used were 0, 0.4, 0.8, 1.2, 1.6, and 2.0 M. These were monitored at 225 nm with an equilibration time of 0 and 0.5 min for both calcium conditions. The shape and position of the curve were not dependent on the equilibration time.

(B) Differential Scanning Calorimetry. Heat-induced unfolding was performed in a Nano II DSC (Calorimetry Sciences Corp.) fitted with a capillary cell. The experiments were done under two sets of conditions. First, in the absence of calcium (apo), MECAD12 (26 μM stock) was dialyzed under stringent reducing conditions. The buffer used was 10 mM potassium phosphate, 140 mM NaCl, and 1 mM TCEP, pH 7.4, with nitrogen gas bubbling through the dialysis in order to replace the oxygen present. In the presence of calcium, MECAD12 (26 μM stock) was dialyzed against 140 mM NaCl, 2 mM HEPES, 1 mM TCEP, and 1 mM $CaCl_2$, pH 7.4, under similarly stringent reducing conditions. After dialysis, the protein concentrations for these experiments were determined by UV absorbance from baselines that were corrected for scattering. All of the samples were degassed for 2 min at room temperature prior to loading the cell. The scan rate was 1 °C/min. Protein concentrations were 0.5 and 2.0 mg/mL for 1 mM Ca^{2+} and apo conditions, respectively. UV scans were also taken for protein solutions removed from the capillary cells after performing each DSC scan in order to check for any change in concentration and light scattering. Protein solutions from before and after DSC temperature scans yielded identical UV spectra.

Unfolding Studies: Urea-Induced Denaturation. Isothermal Manual Titration As Monitored by CD. Constant volume urea denaturations were performed manually in the absence (apo; 10 μM EGTA) and presence of calcium (1 mM). Urea titrations in the apo condition were performed at 25 °C. For apo−urea titrations the native buffer was 140 mM NaCl, 2 mM HEPES, 1 mM TCEP, and 10 μM EGTA, pH 7.4, with a protein concentration of 5 μM. The urea titrant reservoir contained the same buffer and protein concentration as in the native solution with the addition of ~9 M urea. Titrations in the presence of calcium were done at 30 °C. Native buffer was 140 mM NaCl, 2 mM HEPES, 1 mM TCEP, and 1 mM $CaCl_2$ with a protein concentration of 5 μM. Urea was of ultrapure quality (Nacalai Tesque Inc., Kyoto, Japan). Urea concentration was determined using a Bausch and Lomb refractrometer (*38*).

Wavelength scans from 300 to 200 nm were taken for each addition using circular dichroism with an averaging time of 5 s. A quartz cuvette with a path length of 4 mm was used for all titrations with constant stirring during measurements. The minimum signal was at approximately 217 nm but had a poor signal-to-noise ratio due to buffer absorption. Thus, results at ellipticity values of 222 and 235 nm were reported.

Data Analysis. Data were analyzed using IGOR Pro (version 4.0; Wavemetrics), with procedure files written in-house. Temperature-induced unfolding transitions monitored by CD were fit to a two-state unfolding model represented as

$$\text{native} \leftrightarrow \text{unfolded} \quad (1)$$

The equilibrium constant, K, is given by

$$K = [\mathrm{U}]/[\mathrm{N}] \tag{2}$$

The mole fraction of the unfolded species is given by

$$f_{\mathrm{U}} = \frac{K}{1+K} \qquad K = \mathrm{e}^{-\Delta G/RT} \tag{3}$$

The relationship between free energy change and melting temperature is given by the equation

$$\Delta G = \Delta H_{\mathrm{m}}\left(1 - \frac{T}{T_{\mathrm{m}}}\right) + \Delta C_p\left(T - T_{\mathrm{m}} - T\ln\frac{T}{T_{\mathrm{m}}}\right) \tag{4}$$

where ΔH_{m} is the enthalpy of unfolding at the melting temperature, T_{m} is the melting temperature, and ΔC_p is the heat capacity at the melting temperature (*39*). Unfolding data from the CD were fit to eqs 3 and 4 with baseline slopes and intercepts as fitted parameters. The CD signal between 240 and 215 nm decreased upon unfolding.

Temperature denaturation data from CD for the apo condition were also analyzed using a three-state unfolding model according to the equilibrium

$$\text{native} \overset{K_1}{\longleftrightarrow} \text{intermediate} \overset{K_2}{\longleftrightarrow} \text{unfolded} \tag{5}$$

The equilibrium constants, K_1 and K_2, are given by

$$K_1 = [\mathrm{I}]/[\mathrm{N}] \qquad K_2 = [\mathrm{U}]/[\mathrm{I}] \tag{6}$$

such that the individual transitions are two state. Mole fractions for each species are given by the equations

$$f_{\mathrm{U}} = \frac{K_1K_2}{1 + K_1 + K_1K_2}$$

$$f_{\mathrm{I}} = \frac{K_1}{1 + K_1 + K_1K_2}$$

$$f_{\mathrm{N}} = 1 - f_{\mathrm{I}} - f_{\mathrm{U}} \tag{7}$$

Experimentally, the signal of the two domain construct, MECAD12, was twice that of L1-ECAD2-L2. This indicates that half of the CD signal in MECAD12 is due to domain 1 and half due to domain 2. The sensitivity of resolved parameters to the value of ΔC_p was tested by fixing it to integer values from 0 to 3 kcal/(mol·K). The value for χ^2 decreased as ΔC_p was increased. ΔH_{m} decreased only by 1 kcal/mol, and T_{m} decreased only by 0.05 °C for this range of ΔC_p. Values resolved for fits with ΔC_p fixed to 0 kcal/(mol·K) are reported in Table 1.

Resolved enthalpies and melting temperatures were fit to a linear equation to give a Kirchoff plot (Figure 4C). The slope provides an estimate of ΔC_p of unfolding according to the equation

$$\Delta C_p = \delta\Delta H_{\mathrm{m}}/\delta T_{\mathrm{m}} \tag{8}$$

For denaturant-induced unfolding, ΔG is given by

$$\Delta G = \Delta G^\circ - m_{\mathrm{G}}[\mathrm{D}] \tag{9}$$

where ΔG° is free energy of unfolding of protein in the absence of denaturant and m_{G} is the sensitivity of the protein to the concentration of denaturant, [D] (*40*, *41*).

Table 1: Results from Temperature Denaturation of MECAD12[a]

log([Ca^{2+}])	ΔH_{m} (kcal/mol)	T_{m} (°C)	ΔG° at 25 °C[c] (kcal/mol)
−9 (apo)	40.0 ± 1.5	41.6 ± 0.2	2.1 ± 0.3 (1.0)
−9[b] (transition 1)	40 ± 2	38.8 ± 0.5	1.8 ± 0.3 (ND)
−9[b] (transition 2)	38 ± 2	45.1 ± 0.5	2.4 ± 0.3 (1.6)
−6	38 ± 2	42.4 ± 0.4	2.1 ± 0.3 (0.8)
−4	70 ± 2	45.8 ± 0.1	4.6 ± 0.1 (3.9)
−3	117 ± 4	57.20 ± 0.08	11.4 ± 0.3 (9.8)
−2	120 ± 7	65.1 ± 0.2	14.2 ± 0.3 (11.8)

[a] Results of fits to eqs 3 and 4 with ΔC_p fixed to 0. [b] Results of fits to eqs 6 and 7 with both ΔC_p values fixed to 0. [c] Values reported with errors are calculated on the basis of fits in which ΔC_p was fixed to 0 kcal/(mol·K). Values in parentheses were calculated on the basis of ΔC_p obtained from Kirchoff plots (Figure 4C). For apo and 1 μM Ca^{2+} conditions, ΔC_p was 2.6 kcal/(mol·K). For transition 2 of the apo condition, ΔC_p was 1.3 kcal/(mol·K) (*34*). For 0.1−10 mM Ca^{2+} conditions, ΔC_p was 1.0 kcal/(mol·K).

DSC data were processed using the program $C_p$calc provided with the Nano II DSC that converts power readings (microwatts) to molar heat capacity using the concentration and molecular weight of MECAD12, the volume of the cell (0.3 mL), and the partial specific volume of the protein, 0.73 mL/g. Baselines were fit to either a polynomial or linear baseline as seemed appropriate.

Binding constants were estimated by fitting all calcium-dependent, temperature-denaturation data monitored by CD to the equation

$$f_{\mathrm{U}} = \frac{[\mathrm{U}]}{[\mathrm{U}] + [\mathrm{N_{apo}}] + [\mathrm{N_1}] + [\mathrm{N_2}] + [\mathrm{N_3}]} \tag{10}$$

where the four native species are the apo, singly, doubly, and triply bound forms of the protein. We assumed that calcium-binding sites in MECAD12 were equal and independent given by the binding equation

$$\mathrm{N_{apo}} + n\mathrm{Ca}^{2+} \overset{K^n}{\longleftrightarrow} \mathrm{N}_n \tag{11}$$

where n is the number of ligands and K is the equilibrium constant for binding of one ligand. [U] is given by eqs 2−4. We assumed that the unfolded state did not bind calcium. Data were first normalized to the end points of the individual fits to the unfolding transitions and then fitted to eq 10 to return an estimate for the binding constant. The data did not support a more sophisticated model for ligand association to the native state of MECAD12.

RESULTS

UV and CD Spectra. The UV spectrum showed a typical tryptophan-containing protein with a local maximum at 280 nm and a shoulder at 290 nm (Figure 2A). The CD spectra had a wavelength minimum at approximately 216 nm (Figure 2B) as typical for a β-sheet protein. The CD spectra in the presence and absence of calcium showed a slight change in the signal between 212 and 235 nm. There was a decrease in the CD signal upon adding calcium, indicating a conformational change in the protein as a function of calcium.

Temperature Denaturation. A plot of normalized CD signal at 225 nm versus temperature was generated from

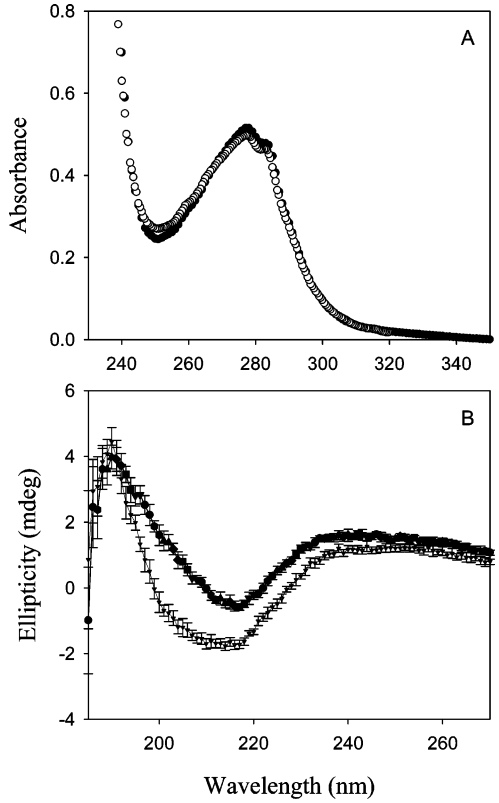

FIGURE 2: Spectra of MECAD12. (A) UV spectra of MECAD12 (~20 μM) in the absence (10 μM EGTA, 140 mM NaCl, 20 mM potassium phosphate, 1 mM TCEP, pH 7.4) and presence (1 mM $CaCl_2$, 140 mM NaCl, 2 mM HEPES, 1 mM TCEP, pH 7.4) of calcium. Spectra were corrected for baseline offset. (B) CD spectra (in mdeg) of 16 μM MECAD12 from 200 to 290 nm (0.2 mm path length) in low and high calcium. The buffer for the low calcium condition is 2 mM HEPES and 140 mM NaCl, pH 7.4, and for the high calcium condition is 2 mM HEPES, 140 mM NaCl, and 5 mM $CaCl_2$, pH 7.4.

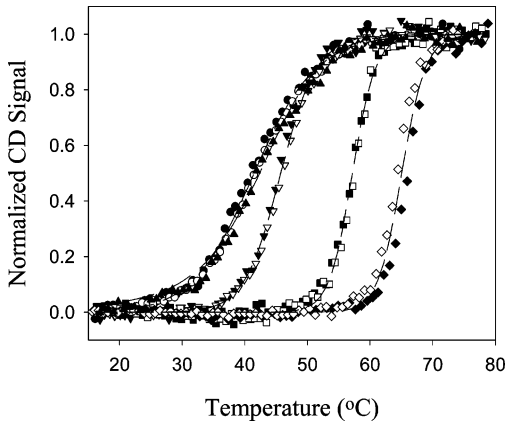

FIGURE 3: Plot of the normalized CD signal versus temperature (°C) from temperature denaturation of MECAD12 (10 μM) at five different calcium conditions. For each calcium condition, two data sets have been plotted. Symbols: apo (●, ○), 1 μM calcium (▲, △), 100 μM calcium (▼, ▽), 1 mM calcium (■, □), and 10 mM calcium (◆, ◇). Solid lines are simulated curves based on parameters resolved from fits to eqs 3 and 4 in which ΔC_p was fixed to 0 kcal/(mol·K).

temperature-denaturation experiments at different calcium concentrations (Figure 3). The solid lines are simulated on the basis of the parameters resolved from fits to the two-state model with ΔC_p fixed to zero. Resolved values for ΔH_m and T_m and calculated values for $\Delta G°$ at 25 °C (eq 4) are reported in Table 1. There was no significant difference between data in 10 μM EGTA and 1 μM calcium as reflected in the resolved parameters for fits to the two-state model for these two calcium conditions. The slopes for apo and 1 μM calcium were shallow compared to the calcium-added data sets. Thus, upon addition of calcium, the transitions progressed toward higher T_m and higher values of ΔH_m.

The shallow transition for the apoprotein and the modular domain structure led to the exploration of a three-state model of unfolding (eq 5). Parameters resolved from these fits are reported in Table 1. The T_m for the first transition (38.8 °C) is 6 °C less than that of the second transition (45 °C). The enthalpies for each transition are the same (40 kcal/mol) and equal to the enthalpy resolved from fits to the two-state model. The span and randomness of the residuals were equivalent in the fits to the two- and three-state models.

To get an estimate of the ΔC_p, a series of temperature-denaturation experiments were performed with addition of low levels of urea. Figure 4 shows plots of normalized CD signal versus temperature for apo-MECAD12 (panel A) and MECAD12 in 1 mM calcium (panel B). The T_m decreased with the increase in urea concentration. The apo transitions did not have well-defined native baselines, indicating that the protein was easily denatured in the absence of calcium (Figure 4A). (The value for the slope of the native baseline was fixed to zero to resolve the parameters illustrated in Figure 4C.) In the presence of calcium all transitions shifted to higher temperature and were steeper and had well-defined baselines. The data were fit to the two-state model, and resolved values for ΔH_m and T_m were plotted in Figure 4C. The relative error on ΔH_m was the same in the two calcium concentrations. From the slope of these data sets, we estimated ΔC_p for apo to be 2.6 ± 0.6 kcal/(mol·K) and 1.0 ± 0.3 kcal/(mol·K) for the protein in 1 mM calcium. On the basis of these estimates of ΔC_p, values for $\Delta G°$ were calculated and reported in Table 1 (values in parentheses). From the MECAD12 structure (*8*) with calcium bound, we used sracer (*42*) to calculate the ΔC_p according to Livingstone et al. (*43*) to be ~1.85 kcal/(mol·K). A similar calculation of ΔC_p according to Myers et al. (*44*) returned 2.5 kcal/(mol·K). The experimental value is 1.0 ± 0.3 kcal/(mol·K) for the calcium-bound state. It is possible that MECAD12 is not completely extended in the unfolded state, leading to an overestimation of computed values for ΔC_p. This discrepancy could also be due to calcium association with cadherin in the unfolded state.

MECAD12 was subjected to denaturation using differential scanning calorimetry in the presence and absence of calcium at two different concentrations of protein, each under stringently reduced conditions. Figure 5 shows the scans of MECAD12 taken in DSC in the absence of calcium (10 μM EGTA) and 1 mM calcium conditions. The data shown in Figure 5 were corrected for a linear native baseline. We see a shift in the midpoint of transition curve from ~41 °C for apo to ~57 °C for 1 mM calcium conditions. These values are consistent with the T_m values obtained from temperature-denaturation experiments monitored by CD. Values for ΔH_{cal} were determined by forcing ΔC_p to be 0 kcal/(mol·K). Fitted enthalpies were to a two-state model. Resolved values for ΔH_{vH} and ΔH_{cal} were similar such that their ratio was approximately 1 and returned values of ~80 kcal/mol for the apo state and 120 kcal/mol for the 1 mM calcium

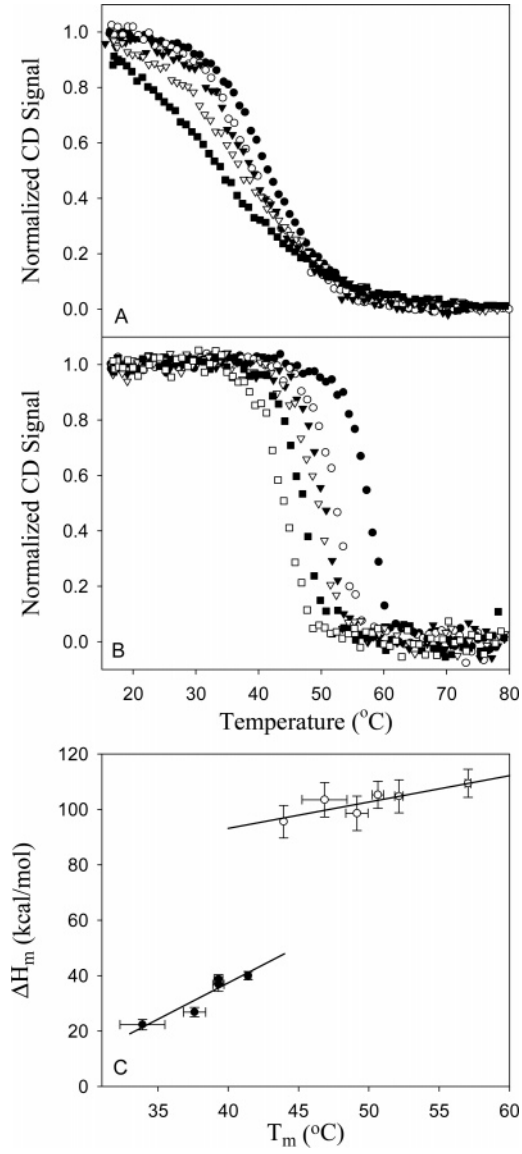

FIGURE 4: Temperature-induced unfolding of MECAD12 in the presence of urea in apo and 1 mM calcium conditions. (A) Plot of the normalized CD signal (mdeg; 225 nm) against temperature (°C) for MECAD12 in the apo condition. Symbols are data taken with 0 M (●), 0.2 M (○), 0.4 M (▼), 0.6 M (▽), and 0.8 M (■) urea added. (B) Plot of the normalized CD signal (mdeg, 225 nm) against temperature (°C) for MECAD12 in the 1 mM calcium condition. Symbols are data taken with 0 M (●), 0.4 M (○), 0.8 M (▼), 1.2 M (▽), 1.6 M (■), and 2.0 M (□) urea added. (C) Van't Hoff enthalpy is plotted against the melting temperature (°C). Values were resolved from fits of the data (panels A and B) to the Gibbs−Helmholz equation in which ΔC_p was fixed to 0 [apo (●) and 1 mM Ca^{2+} (○)]. The slope of the best-fit line to the data is 2.6 ± 0.6 kcal/(mol·K) for the apo condition and 1.0 ± 0.3 kcal/(mol·K) for the 1 mM calcium condition.

condition. Despite the close agreement with the results reported in Table 1, we have limited confidence in these values due to poor definition of the unfolded baselines (see Discussion).

Reversibility. Initial experiments were performed to address the issue of reversibility of the unfolding transitions of MECAD12. Solutions of apo-MECAD12 that had been unfolded were refolded, and the CD signal was monitored at 225 nm. There was a clear hysteresis during refolding such that the refolding lagged the unfolding curve at a given

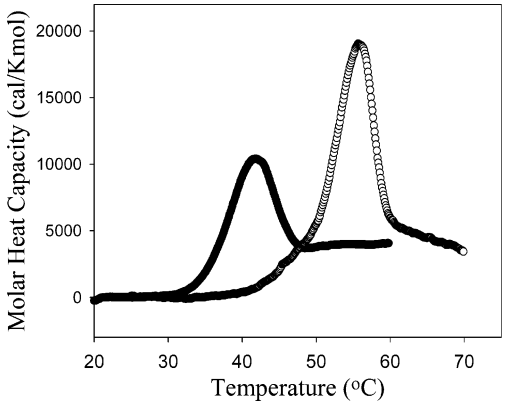

FIGURE 5: Molar heat capacity [cal/(mol·K)] is plotted against the temperature (°C) for thermal denaturation of MECAD12 monitored by differential scanning calorimetry. Symbols represent the thermal transition curve (●) in the apo condition (10 μM EGTA) and (○) for the 1 mM calcium condition.

temperature (data not shown). This is consistent with the refolding experiments on the domain 2 constructs with linkers attached [T_m (L1-ECAD2-L2) = 45 °C (*35*)] and in contrast to the denaturation of core domain 2 where the unfolding and refolding curves overlayed [T_m = 54 °C (*34*)]. These results are consistent with the explanation that the four *cis*-X-proline bonds (Figure 1C) are responsible for the slow refolding of the domains (two *cis*-X-proline bonds in each domain).

Estimation of the Calcium-Binding Constant. Binding constants for calcium were estimated in two ways from the calcium-dependent shifts in the denaturation profiles. Both analyses assumed that the protein bound three ligands independently and with identical affinity. Simultaneous analysis of data shown in Figure 3 according to eqs 10 and 11 resolved a value of 18000 ± 1000 M^{-1}. The fits did not accommodate the differences in the slopes of the unfolding transitions as a function of calcium concentration. Thus, although the midpoints were well fitted in the simultaneous analysis, the shapes were not. The calcium-binding affinity was also estimated by piecewise analysis of the transitions (*45*), yielding a value of 46000 ± 37000 M^{-1}.

Urea Denaturation Experiments. Urea denaturation experiments in apo and 1 mM calcium conditions were performed manually. Figure 6 shows the normalized CD signal versus urea concentration in apo (25 °C) and 1 mM calcium (30 °C) conditions. In the presence of calcium, the midpoint of the transition shifted to a higher concentration of urea, indicating stabilization of protein by calcium. The data were fitted to eqs 3 and 9 in order to resolve $\Delta G°$ and m_G for apo and for 1 mM calcium conditions. The resolved parameters are reported in Table 2. Values for $\Delta G°$ from temperature-denaturation studies are shown to aid in comparison of these two experiments. These values are dependent upon the value for ΔC_p and required extrapolation from the melting temperature to the temperature of the urea-denaturation experiments. Since the 1 mM Ca^{2+} data required a longer extrapolation, there is closer agreement between the values for free energy for the apo experiments and less agreement for the 1 mM calcium experiments. According to Myers (*44*), the calculated m_G (urea) is 1.99 kcal/(mol·M), a value close to the experimental value of 1.8 ± 0.2 kcal/(mol·M) (Table 2).

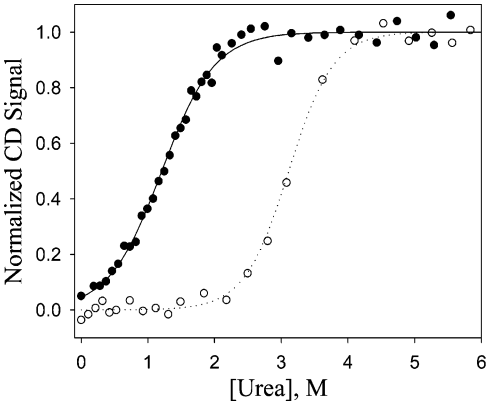

FIGURE 6: Urea denaturation of MECAD12 in the apo and 1 mM calcium conditions. Plot of the normalized CD signal (235 nm) versus molar urea concentration in the apo (●) and 1 mM calcium (○) condition.

Table 2: Results from Urea-Induced Unfolding of MECAD12

conditions	$\Delta G°$ (T_m) (kcal/mol)	$\Delta G°$ (urea) (kcal/mol)	m_G [kcal/(mol·M)]
apo[a]	2.1 ± 0.3[c]	1.8 ± 0.1	1.5 ± 0.1
1 mM Ca^{2+} [b]	8.5 ± 1.2[d]	5.6 ± 0.6	1.8 ± 0.2

[a] 25 °C. [b] 30 °C. [c] ΔC_p fixed to 0 kcal/(mol·K). [d] ΔC_p fixed to 1 kcal/(mol·K).

DISCUSSION

Although the extracellular region of epithelial cadherin is comprised of modular domains, they must cooperate in order to transduce the signal of adhesion into the cytoplasm of the cell. The calcium that binds at the interface between the modular domains necessarily links them energetically and structurally. Interestingly, we find that, despite their modular structure, the domains are energetically coupled even in the absence of calcium. The following sections discuss the quantitative evaluation of the energetic linkage between stability and calcium binding through analysis of the apo unfolding data, the context dependence of the stability of domain 2, and the effects of calcium upon the unfolding transitions.

Model-Dependent Analysis of the Apo Unfolding Data. The denaturation profiles for the apo species were significantly shallower than for the calcium-bound species such that approximately 30% of the protein was denatured at 37 °C (Figure 3). According to a model that allows for a single transition between the native and unfolded states (eq 1), the melting temperature of the apo transition was approximately 42 °C. Although this construct contains domain 2, the melting temperature was 12 °C less than the isolated ECAD2 (*34*). The value of ΔH_m is 40 kcal/mol for MECAD12, a value that when corrected for the difference in melting temperatures compares well with that for ECAD2. This is surprising given that MECAD12 is twice the size of ECAD2.

The value for ΔC_p resolved from the Kirchoff plot (Figure 4C) can be compared to that determined for ECAD2. Apo-MECAD12 unfolded with a change in heat capacity of 2.6 kcal/(mol·K), a value twice that found for apo-ECAD2 (*34*). This would be predicted given that MECAD12 is twice the size of ECAD2. This interpretation implies that (1) ECAD1 has a similar ΔC_p to ECAD2, (2) ΔC_p is temperature independent, and (3) the heat capacity of the native and unfolded states has the same dependence upon temperature.

The modular structure of the extracellular domain of cadherin is apparent from crystallographic studies (*8*, *21*, *22*). We investigated the possibility of energetic independence of the two domains of MECAD12 through fits of apo transitions to a three-state model (eq 5). This allowed parsing of the temperature-unfolding transition of apo-MECAD12 into the energetic contributions of individual domains. The results from fits to the three-state model showed the following points. First, there was no difference in the slope of the transition when parsed into two transitions (Table 1). This indicated that the slope of the unfolding transition was constant over a wide range of temperature. Provided that the three-state analysis is valid, the total heat absorbed upon unfolding of the two-domain construct would be 80 kcal/mol (sum of two 40 kcal/mol transitions). Second, the resolved T_m values for the two transitions were symmetrically distributed from the T_m for the fit to the two-state model. There was no clear indication of a three-state transition from inspection of the residuals for the fit. The strength in the three-state analysis lies in the fact that transition 2 had an identical T_m to that for L1-ECAD2-L2 (*35*). This is consistent with assigning the unfolding of domain 2 to the second transition in the three-state analysis.

What do we know about the stability of domain 1? Studies in our laboratory of isolated domain 1 (ECAD1) and domain 1 with linker 1 (ECAD1-L1) have been confounded by the low solubility of these constructs (data not shown). Although we have not made a quantitative assessment of the stability of domain 1 constructs, it is clear that it is significantly less stable than the domain 2 constructs. If we assign the first transition from the three-state analysis of apo-MECAD12 to the unfolding of domain 1, the T_m for this domain would be 38 °C. Thus, only half of the domain 1 modules are folded under apo conditions at physiological temperatures.

Spectroscopic data agreed with the results obtained from DSC experiments. T_m for apo-MECAD12 was ~42 °C according to DSC and spectroscopic studies. The enthalpy value resolved from a two-state fit of the DSC data (ΔH_{vH}) was equal to the sum of the enthalpy values of both transitions from the three-state fit to the spectroscopic data (~80 kcal/mol). The DSC endotherm was narrower than a two-state transition in a similar fashion as noted for ECAD2 (*34*). Interpretation of the DSC results in terms of enthalpy is of limited value based on the issues with the unfolded baseline noted previously. In the presence of 1 mM calcium, both T_m and ΔH_{vH} agreed for the spectroscopic and DSC experiments (T_m was ~55 °C; ΔH_{vH} was 120 kcal/mol). We take this as qualitative support for using a three-state model to interpret the apo-MECAD12 unfolding transition.

There was evidence of a second transition at higher temperature in DSC in both low- and high-calcium conditions. In other studies under weakly oxidizing apo conditions, this second transition was distinct from the monomer melting transition and had a calcium-dependent melting temperature (data not shown). We believe this more stable species to be the disulfide-linked dimer through C9 located at the base of strand a and, perhaps, even higher ordered structures. Size exclusion studies indicate that the disulfide-linked dimers form stable higher ordered structures (*46*). Subsequent experiments reported here performed under stringent reducing

Table 3: Context-Dependent Change in Entropy and Enthalpy for Apo Domain 2[a]

context	ΔH_{50} (kcal/mol)	ΔS_{50} [cal/(mol·K)]
ECAD2[b]	85 ± 2 (0.80)	260 ± 9 (2.5)
L1-ECAD2-L2[c]	76.9 ± 2.5 (0.64)	242 ± 8 (2.0)
MECAD12 (transition 2)[d]	42.9 ± 2 (0.40)	135 ± 7 (1.3)

[a] The value of ΔC_p was fixed to 1 kcal/(mol·K) for all data sets to facilitate comparison. All values in parentheses are per residue values obtained by dividing the parameter by the number of residues in the construct. [b] Data from Prasad et al. (*34*); 106 residues. [c] Data from Prasad et al. (*35*); 120 residues. [d] Data reported in Table 1 for transition 2 from three-state analysis; 106 residues for domain 2 only.

conditions still displayed irregularities of the unfolded baseline. This second transition was not apparent in the spectroscopic studies and is likely a consequence of the higher concentration of protein required for DSC measurements.

Context-Dependent Behavior. Studies of the isolated core domain 2 (ECAD2) showed that it is quite stable even in the absence of calcium and it is monomeric (*34*). These studies were extended to see the effect of adjoining linkers on the stability of ECAD2 (*35*). We learned the following lessons from these studies. First, ECAD2 is destabilized by the addition of the adjoining linker segments when added piecewise to the N- and C-terminus. [The domain 2 construct with both of the adjacent linkers (L1-ECAD2-L2) was destabilized by 9 °C.] Second, the constructs were stabilized by salt such that the destabilization of ECAD2 by the linkers could be explained by electrostatic repulsion.

This paper reports the calcium-dependent stability of MECAD12, a construct that is one step more sophisticated than L1-ECAD2-L2 in that it contains domain 1, as well. Despite the apparent modular structure of MECAD12, this construct denatured in a single shallow transition as discussed previously. The second transition from three-state analysis can be compared to previous work on domain 2 (ECAD2) to illustrate the impact of domain 1 and the linker segments upon the stability of domain 2. A major finding in the studies reported here is that the stability of domain 2 in the MECAD12 construct (2.4 kcal/mol, 25 °C) is less than when placed in the context of its adjoining linkers only [L1-ECAD2-L2, 4.0 kcal/mol (*35*)] or as the isolated core domain 2 [ECAD2, 6.6 kcal/mol (*34*)].

To further evaluate the context-dependent behavior of domain 2, we calculated the enthalpy and entropy at a common temperature close to the T_m. This allows comparison between the three contexts of domain 2 with minimal dependence upon ΔC_p. Table 3 reports values for ΔH and ΔS at 50 °C. There is a clear trend toward decreasing enthalpy as the sophistication of the context increases. There is a substantial decrease in enthalpy when domain 2 is in the context of MECAD12 (presence of domain 1). The trend in enthalpy is consistent with the decrease in stability. Entropy also decreases as the sophistication of the context increases in apparent opposition to the decrease in stability. The decreasing value of ΔS_{50} may reflect an increase in entropy of the native state as the sophistication of the context increases.

The destabilization of the core domain for our domain 2 constructs is unusual as observed by review of relevant literature for domains of similar size as ECAD2 (*35*). In brief, titin modules (*47*, *48*), the fibronectin type III domain from tenascin (*49*), the tryptic fragment of microsomal cytochrome b_5 (*50*), and the N-terminal domain of *Paramecium* calmodulin (*51*, *52*) showed increased stability with addition of adjacent segments. Placek and Gloss (*53*) reported that the stability of the histone 2 dimer (WT-H2A/H2B) is stabilized when the N-terminal tail of H2A is present, yet is *destabilized* when the N-terminal tail of H2B is present. Thus, we found only a single example in the literature of destabilization of a core domain from addition of adjacent segments.

Calcium Binding to MECAD12. There were several pieces of evidence that MECAD12 bound calcium. MECAD12 spectral characterization shows minimum ellipticity at about 216 nm that is a typical for proteins with dominating β-sheet conformation (Figure 2) (*54*, *55*). In the presence of calcium the CD signal decreased (less negative), indicating that the conformation of MECAD12 is sensitive to calcium (*56*, *57*). The unfolding transitions shifted to higher temperature as the concentration of calcium increased, indicating that the protein is stabilized by calcium (Figure 3). The denaturant-induced unfolding transitions shifted to higher urea concentration in the presence of 1 mM calcium (Figure 6). Thus, experimental evidence supports the conclusion that calcium binds and stabilizes the MECAD12 construct.

A calcium-binding constant can be derived from the calcium-dependent displacement of the temperature-induced unfolding transitions (Figure 3). The discussion of linked equilibria is well established in the literature (*45*, *58*). This approach was used to determine the energetics of binding of cytidine 2′-monophosphate to ribonuclease A using calorimetry (*59*) and calcium binding to mutants of the C-terminal domain of calmodulin from urea denaturation profiles (*60*). Using this approach, we found a dissociation constant of 22−55 μM.

There have been several studies of the calcium-binding affinity of the extracellular domains of cadherin. The Ca^{2+}-binding studies by flow dialysis for ECAD1 by Tong et al. yielded a K_d of 160 μM for Ca^{2+} (*57*) with a stoichiometric ratio of 1 for binding to a construct containing 145 amino acids (ECAD1, linker 1, plus approximately half of ECAD2). Calcium titrations were monitored for MECAD12 using flow dialysis and tryptophan fluorescence for protein concentrations ranging from 1.5 to 50 μM (*61*). The data showed that at MECAD12 concentrations with roughly equal populations monomeric and dimeric forms of calcium bound with a stoichiometry of three ions per polypeptide chain and K_d of 23 μM. These values were significantly higher affinity than the value obtained by Koch et al. (MECAD12, 330 μM) (*56*). The Hill coefficient for Ca^{2+} binding increased from 1.5 to 2.4 with the increase in protein concentration, showing that dimer formation contributed to the cooperativity in Ca^{2+} binding (*61*). Direct titration of 84 kDa epithelial cadherin (ECAD1−5) monitored spectroscopically yielded average K_d values of 45−150 μM with a Hill coefficient of 1.8 (*33*). Thus, the derived binding constant from the experiments reported here agreed well with values determined for various extracellular constructs of E-cadherin reported in the literature.

The calcium-binding affinity for MECAD12 is dependent on the presence of both domains. Studies of L1-ECAD2 and L1-ECAD2-L2 (*35*) reported an apparent binding constant

of 1000 M^{-1} derived from the calcium-dependent shift in denaturation profiles. This value is significantly less than that reported here for MECAD12. Thus, the presence of domain 1 is essential to create the calcium-binding environment at the interface between the two domains (Figure 1B).

In summary, the modular domains of epithelial cadherin exhibit context-dependent behavior in both the apo and calcium-bound states. Our studies suggest that there is interaction between the domains such that the unfolding profile of MECAD12 is not simply the sum of the unfolding profiles for domains 1 and 2. At this stage it is hard to interpret the physiological implications of these studies. However, current studies reflect that the modular structures function as a cooperative unit. This cooperativity between the modules is consistent with the physiological role of epithelial cadherin in signal transduction through cell-adhesive contacts.

REFERENCES

1. Ringwald, M., Schuh, R., Vestweber, D., Eistetter, H., Lottspeich, F., Engel, J., Dolz, R., Jahnig, F., Epplen, J., Mayer, S., et al. (1987) The structure of cell adhesion molecule uvomorulin. Insights into the molecular mechanism of Ca^{2+}-dependent cell adhesion, *EMBO J. 6*, 3647−3653.
2. Takeichi, M. (1991) Cadherin cell adhesion receptors as a morphogenetic regulator, *Science 251*, 1451−1455.
3. Vleminckx, K., and Kemler, R. (1999) Cadherins and tissue formation: integrating adhesion and signaling, *BioEssays 21*, 211−220.
4. Alattia, J. R., Kurokawa, H., and Ikura, M. (1999) Structural view of cadherin-mediated cell−cell adhesion, *Cell. Mol. Life Sci. 55*, 359−367.
5. Nollet, F., Kools, P., and van Roy, F. (2000) Phylogenetic analysis of the cadherin superfamily allows identification of six major subfamilies besides several solitary members, *J. Mol. Biol. 299*, 551−572.
6. Yagi, T., and Takeichi, M. (2000) Cadherin superfamily genes: functions, genomic organization, and neurologic diversity, *Genes Dev. 14*, 1169−1180.
7. Chothia, C., and Jones, E. Y. (1997) The molecular structure of cell adhesion molecules, *Annu. Rev. Biochem. 66*, 823−862.
8. Nagar, B., Overduin, M., Ikura, M., and Rini, J. M. (1996) Structural basis of calcium-induced E-cadherin rigidification and dimerization, *Nature 380*, 360−364.
9. Tomschy, A., Fauser, C., Landwehr, R., and Engel, J. (1996) Homophilic adhesion of E-cadherin occurs by a co-operative two-step interaction of N-terminal domains, *EMBO J. 15*, 3507−3514.
10. Hynes, R. O. (1999) Cell adhesion: old and new questions, *Trends Cell Biol. 9*, M33−M37.
11. Adams, C. L., and Nelson, W. J. (1998) Cytomechanics of cadherin-mediated cell−cell adhesion, *Curr. Opin. Cell Biol. 10*, 572−577.
12. Bienz, M., and Hamada, F. (2004) Adenomatous polyposis coli proteins and cell adhesion, *Curr. Opin. Cell Biol. 16*, 528−535.
13. Barth, A. I., Nathke, I. S., and Nelson, W. J. (1997) Cadherins, catenins and APC protein: interplay between cytoskeletal complexes and signaling pathways, *Curr. Opin. Cell Biol. 9*, 683−690.
14. Ben-Ze'ev, A., and Geiger, B. (1998) Differential molecular interactions of beta-catenin and plakoglobin in adhesion, signaling and cancer, *Curr. Opin. Cell Biol. 10*, 629−639.
15. Overduin, M., Harvey, T. S., Bagby, S., Tong, K. I., Yau, P., Takeichi, M., and Ikura, M. (1995) Solution structure of the epithelial cadherin domain responsible for selective cell adhesion, *Science 267*, 386−389.
16. Overduin, M., Tong, K. I., Kay, C. M., and Ikura, M. (1996) ^{1}H, ^{15}N and ^{13}C resonance assignments and monomeric structure of the amino-terminal extracellular domain of epithelial cadherin, *J. Biomol. NMR 7*, 173−189.
17. Alattia, J. R., Tong, F. K., Tong, K. I., and Ikura, M. (2000) Sequence-specific resonance assignments and partial unfolding of extracellular domains II and III of E-cadherin, *J. Biomol. NMR 16*, 181−182.
18. Haussinger, D., Ahrens, T., Sass, H. J., Pertz, O., Engel, J., and Grzesiek, S. (2002) Calcium-dependent homoassociation of E-cadherin by NMR spectroscopy: changes in mobility, conformation and mapping of contact regions, *J. Mol. Biol. 324*, 823−839.
19. Haussinger, D., Ahrens, T., Aberle, T., Engel, J., Stetefeld, J., and Grzesiek, S. (2004) Proteolytic E-cadherin activation followed by solution NMR and X-ray crystallography, *EMBO J. 23*, 1699−1708.
20. Boggon, T. J., Murray, J., Chappuis-Flament, S., Wong, E., Gumbiner, B. M., and Shapiro, L. (2002) C-cadherin ectodomain structure and implications for cell adhesion mechanisms, *Science 296*, 1308−1313.
21. Pertz, O., Bozic, D., Koch, A. W., Fauser, C., Brancaccio, A., and Engel, J. (1999) A new crystal structure, Ca^{2+} dependence and mutational analysis reveal molecular details of E-cadherin homoassociation, *EMBO J. 18*, 1738−1747.
22. Tamura, K., Shan, W. S., Hendrickson, W. A., Colman, D. R., and Shapiro, L. (1998) Structure−function analysis of cell adhesion by neural (N-) cadherin, *Neuron 20*, 1153−1163.
23. Shapiro, L., Fannon, A. M., Kwong, P. D., Thompson, A., Lehmann, M. S., Grubel, G., Legrand, J. F., Als-Nielsen, J., Colman, D. R., and Hendrickson, W. A. (1995) Structural basis of cell−cell adhesion by cadherins, *Nature 374*, 327−337.
24. Richardson, J. S. (1977) beta-Sheet topology and the relatedness of proteins, *Nature 268*, 495−500.
25. Bork, P., Holm, L., and Sander, C. (1994) The immunoglobulin fold. Structural classification, sequence patterns and common core, *J. Mol. Biol. 242*, 309−320.
26. Clarke, J., Cota, E., Fowler, S. B., and Hamill, S. J. (1999) Folding studies of immunoglobulin-like beta-sandwich proteins suggest that they share a common folding pathway, *Struct. Folding Des. 7*, 1145−1153.
27. Shapiro, L., Kwong, P. D., Fannon, A. M., Colman, D. R., and Hendrickson, W. A. (1995) Considerations on the folding topology and evolutionary origin of cadherin domains, *Proc. Natl. Acad. Sci. U.S.A. 92*, 6793−6797.
28. Bagby, S., Harvey, T. S., Eagle, S. G., Inouye, S., and Ikura, M. (1994) Structural similarity of a developmentally regulated bacterial spore coat protein to beta gamma-crystallins of the vertebrate eye lens, *Proc. Natl. Acad. Sci. U.S.A. 91*, 4308−4312.
29. Bagby, S., Go, S., Inouye, S., Ikura, M., and Chakrabartty, A. (1998) Equilibrium folding intermediates of a Greek key beta-barrel protein, *J. Mol. Biol. 276*, 669−681.
30. Nose, A., Tsuji, K., and Takeichi, M. (1990) Localization of specificity determining sites in cadherin cell adhesion molecules, *Cell 61*, 147−155.
31. Shan, W. S., Koch, A., Murray, J., Colman, D. R., and Shapiro, L. (1999) The adhesive binding site of cadherins revisited, *Biophys. Chem. 82*, 157−163.
32. Ozawa, M., Engel, J., and Kemler, R. (1990) Single amino acid substitutions in one Ca^{2+} binding site of uvomorulin abolish the adhesive function, *Cell 63*, 1033−1038.
33. Pokutta, S., Herrenknecht, K., Kemler, R., and Engel, J. (1994) Conformational changes of the recombinant extracellular domain of E-cadherin upon calcium binding, *Eur. J. Biochem. 223*, 1019−1026.
34. Prasad, A., Housley, N. A., and Pedigo, S. (2004) Thermodynamic stability of domain 2 of epithelial cadherin, *Biochemistry 43*, 8055−8066.
35. Prasad, A., Zhao, H., Rutherford, J. M., Housley, N. A., Nichols, C., and Pedigo, S. (2005) Effect of linker segments upon the stability of epithelial-cadherin domain 2, *Proteins* (in press).
36. Pace, C. N., Vajdos, F., Fee, L., Grimsley, G., and Gray, T. (1995) How to measure and predict the molar extinction coefficient of a protein, *Protein Sci. 4*, 2411−2423.
37. Gill, S. J., and von Hippel, P. H. (1989) Calculation of protein extinction coefficients from amino acid sequence data, *Anal. Biochem. 182*, 319−326.
38. Pace, C. N. (1986) Determination and analysis of urea and guanidine hydrochloride denaturation curves, *Methods Enzymol. 131*, 266−280.
39. Privalov, P. L. (1979) Stability of proteins: small globular proteins, *Adv. Protein Chem. 33*, 167−241.
40. Santoro, M. M., and Bolen, D. W. (1988) Unfolding free energy changes determined by the linear extrapolation method. 1. Unfolding of phenylmethanesulfonyl alpha-chymotrypsin using different denaturants, *Biochemistry 27*, 8063−8068.

41. Greene, R. F., Jr., and Pace, C. N. (1974) Urea and guanidine hydrochloride denaturation of ribonuclease, lysozyme, alpha-chymotrypsin, and beta-lactoglobulin, *J. Biol. Chem. 249*, 5388−5393.
42. Tsodikov, O. V., Record, M. T., Jr., and Sergeev, Y. V. (2002) A novel computer program for fast and exact calculation of accessible and molecular surface areas and average surface curvature, *J. Comput. Chem. 23*, 600−609.
43. Livingstone, J. R., Spolar, R. S., and Record, M. T., Jr. (1991) Contribution to the thermodynamics of protein folding from the reduction in water-accessible nonpolar surface area, *Biochemistry 30*, 4237−4244.
44. Myers, J. K., Pace, C. N., and Scholtz, J. M. (1995) Denaturant *m* values and heat capacity changes: relation to changes in accessible surface areas of protein unfolding, *Protein Sci. 4*, 2138−2148 [erratum: (1996) *Protein Sci. 5*, 981].
45. Schellman, J. A. (1975) Macromolecular binding, *Biopolymers 14*, 999−1018.
46. Makagiansar, I. T., Nguyen, P. D., Ikesue, A., Kuczera, K., Dentler, W., Urbauer, J. L., Galeva, N., Alterman, M., and Siahaan, T. J. (2002) Disulfide bond formation promotes the cis- and trans-dimerization of the E-cadherin-derived first repeat, *J. Biol. Chem. 277*, 16002−16010.
47. Politou, A. S., Gautel, M., Joseph, C., and Pastore, A. (1994) Immunoglobulin-type domains of titin are stabilized by amino-terminal extension, *FEBS Lett. 352*, 27−31.
48. Pfuhl, M., Improta, S., Politou, A. S., and Pastore, A. (1997) When a module is also a domain: the role of the N terminus in the stability and the dynamics of immunoglobulin domains from titin, *J. Mol. Biol. 265*, 242−256.
49. Hamill, S. J., Meekhof, A. E., and Clarke, J. (1998) The effect of boundary selection on the stability and folding of the third fibronectin type III domain from human tenascin, *Biochemistry 37*, 8071−8079.
50. Newbold, R. J., Hewson, R., and Whitford, D. (1992) The thermal stability of the tryptic fragment of bovine microsomal cytochrome b_5 and a variant containing six additional residues, *FEBS Lett. 314*, 419−424.
51. Sorensen, B. R., Faga, L. A., Hultman, R., and Shea, M. A. (2002) An interdomain linker increases the thermostability and decreases the calcium affinity of the calmodulin N-domain, *Biochemistry 41*, 15−20.
52. Faga, L. A., Sorensen, B. R., VanScyoc, W. S., and Shea, M. A. (2003) Basic interdomain boundary residues in calmodulin decrease calcium affinity of sites I and II by stabilizing helix-helix interactions, *Proteins 50*, 381−391.
53. Placek, B. J., and Gloss, L. M. (2002) The N-terminal tails of the H2A−H2B histones affect dimer structure and stability, *Biochemistry 41*, 14960−14968.
54. Eftink, M. R., Ionescu, R., Ramsay, G. D., Wong, C. Y., Wu, J. Q., and Maki, A. H. (1996) Thermodynamics of the unfolding and spectroscopic properties of the V66W mutant of staphylococcal nuclease and its 1−136 fragment, *Biochemistry 35*, 8084−8094.
55. Greenfield, N. J., Davidson, B., and Fasman, G. D. (1967) The use of computed optical rotatory dispersion curves for the evaluation of protein conformation, *Biochemistry 6*, 1630−1637.
56. Koch, A. W., Pokutta, S., Lustig, A., and Engel, J. (1997) Calcium binding and homoassociation of E-cadherin domains, *Biochemistry 36*, 7697−7705.
57. Tong, K. I., Yau, P., Overduin, M., Bagby, S., Porumb, T., Takeichi, M., and Ikura, M. (1994) Purification and spectroscopic characterization of a recombinant amino-terminal polypeptide fragment of mouse epithelial cadherin, *FEBS Lett. 352*, 318−322.
58. Eftink, M. R., Anusiem, A. C., and Biltonen, R. L. (1983) Enthalpy−entropy compensation and heat capacity changes for protein−ligand interactions: general thermodynamic models and data for the binding of nucleotides to ribonuclease A, *Biochemistry 22*, 3884−9386.
59. Straume, M., and Freire, E. (1992) Two-dimensional differential scanning calorimetry: simultaneous resolution of intrinsic protein structural energetics and ligand binding interactions by global linkage analysis, *Anal. Biochem. 203*, 259−268.
60. Hobson, K. F., Housley, N. A., and Pedigo, S. (2005) Ligand-linked stability of mutants of the C-domain of calmodulin, *Biophys. Chem. 114*, 43−52.
61. Alattia, J. R., Ames, J. B., Porumb, T., Tong, K. I., Heng, Y. M., Ottensmeyer, P., Kay, C. M., and Ikura, M. (1997) Lateral self-assembly of E-cadherin directed by cooperative calcium binding, *FEBS Lett. 417*, 405−408.
62. Laskowski, R. A., MacArthur, M. W., Moss, D. S., and Thornton, J. N. (1993) PROCHECK: a program to check the stereochemical quality of protein structures, *J. Appl. Crystallogr. 26*, 283−291.

BI0510274